JOURNAL OF GEOPHYSICAL RESEARCH, VOL. 114, G04020, doi:10.1029/2008JG000889, 2009

Dual nitrate isotopes in dry deposition: Utility for partitioning NO_x source contributions to landscape nitrogen deposition

E. M. Elliott,[1,2] C. Kendall,[2] E. W. Boyer,[3] D. A. Burns,[4] G. G. Lear,[5] H. E. Golden,[6] K. Harlin,[7] A. Bytnerowicz,[8] T. J. Butler,[9] and R. Glatz[10]

Received 5 November 2008; revised 6 July 2009; accepted 29 July 2009; published 11 December 2009.

[1] Dry deposition is a major component of total atmospheric nitrogen deposition and thus an important source of bioavailable nitrogen to ecosystems. However, relative to wet deposition, less is known regarding the sources and spatial variability of dry deposition. This is in part due to difficulty in measuring dry deposition and associated deposition velocities. Passive sampling techniques offer potential for improving our understanding of the spatial distribution and sources of gaseous and aerosol N species, referred to here as dry deposition. We report dual nitrate isotopic composition ($\delta^{15}N$ and $\delta^{18}O$) in actively collected dry and wet deposition across the high-deposition region of Ohio, New York, and Pennsylvania. We also present results from initial tests to examine the efficacy of using passive nitric acid collectors as a collection medium for isotopic analysis at a site in New York. Isotopic values in actively collected dry deposition, including particulate nitrate and gaseous nitric acid, are compared with those in wet nitrate deposition and surrounding NO_x emission sources. $\delta^{15}N$ values in dry and wet fractions are highest at the westernmost sites and lowest at the easternmost sites, and stationary source NO_x emissions (e.g., power plants and incinerators) appear to be the primary control on $\delta^{15}N$ spatial variability. In contrast, $\delta^{18}O$ values show a less consistent spatial pattern in dry deposition. Both $\delta^{15}N$ and $\delta^{18}O$ show strong seasonality, with higher values in winter than summer. Seasonal variations in stationary source NO_x emissions appear to be the most likely explanation for seasonal variations in $\delta^{15}N$, whereas seasonal variations in air temperature and solar radiation indicate variable chemical oxidation pathways control $\delta^{18}O$ patterns. Additionally, we demonstrate the utility of passive samplers for collecting the nitric acid (HNO_3) component of dry deposition suitable for isotopic analysis. We observe slight differences in $\delta^{15}N$-HNO_3 values between simultaneous samples collected actively and passively (0.6‰). However, we observe a larger offset in $\delta^{18}O$ values between actively and passively collected samples; the causes for this offset warrant further investigation. Nonetheless, passive sample collection represents a significant cost savings over active sampling techniques and could allow a more extensive understanding of patterns of dry deposition and associated insights to nitrogen sources across landscapes.

Citation: Elliott, E. M., C. Kendall, E. W. Boyer, D. A. Burns, G. G. Lear, H. E. Golden, K. Harlin, A. Bytnerowicz, T. J. Butler, and R. Glatz (2009), Dual nitrate isotopes in dry deposition: Utility for partitioning NO_x source contributions to landscape nitrogen deposition, *J. Geophys. Res.*, *114*, G04020, doi:10.1029/2008JG000889.

1. Introduction

[2] Emissions of nitrogen oxides (NO_x) to the atmosphere contribute to photochemical ozone production, particulate matter formation, and deposition of reactive nitrogen to landscapes. As a consequence of the lifetime of NO_x in the atmosphere (1–2 days), these deleterious effects can take place hundreds of kilometers from the initial point of NO_x emission [*Liang et al.*, 1998; *Neuman et al.*, 2006]. Once emitted to the atmosphere, NO_x is oxidized to highly soluble nitric acid (HNO_3) via several pathways and is subsequently removed from the atmosphere as wet or dry deposition. While

[1]Department of Geology and Planetary Science, University of Pittsburgh, Pittsburgh, Pennsylvania, USA.
[2]U.S. Geological Survey, Menlo Park, California, USA.
[3]School of Forest Resources, Pennsylvania State University, University Park, Pennsylvania, USA.
[4]U.S. Geological Survey, Troy, New York, USA.
[5]U.S. Environmental Protection Agency, Washington, D. C., USA.
[6]U.S. Environmental Protection Agency, Athens, Georgia, USA.
[7]Central Analytical Laboratory, National Atmospheric Deposition Program, Champaign, Illinois, USA.
[8]U.S. Forest Service, Riverside, California, USA.
[9]Cary Institute of Ecosystem Studies and Department of Ecology and Evolutionary Biology, Cornell University, Ithaca, New York, USA.
[10]San Francisco, California, USA.

0148-0227/09/2008JG000889$09.00

"true" dry deposition refers to the transfer of gases and particles to surfaces exposed to the atmosphere [*Hicks et al.*, 1987], hereafter we refer to gaseous concentrations of N measured by CASTNET and passive sampling techniques as "dry deposition" for the sake of convention and in accordance with several decades of previously published research. Although HNO_3 can be recycled back to NO_x, this process is slow relative to wet and dry HNO_3 deposition; thus HNO_3 is often considered the final sink for NO_x [*Morino et al.*, 2006].

[3] While wet deposition is generally the largest component of total nitrogen deposition, particularly in temperate regions characterized by adequate rainfall, dry deposition is the dominant form of N deposition in arid climates, such as the western USA [*Fenn et al.*, 2003], and can contribute 20–50% of N deposition in the eastern USA [*Butler et al.*, 2005]. Dry deposition refers to the direct transfer of gaseous and particulate species to the Earth's surface without the aid of precipitation [*Seinfeld et al.*, 1998]. For nitrogen, dry deposition can include gaseous nitrogen species (HNO_3 vapor, NH_3, NO_2, HONO, NO, peroxyacetyl nitrate (PAN)), or aerosols (particulate NO_3^-, particulate NH_4^+). Nitrate in rain and snow can be scavenged from particulate NO_3^- ($NO_{3\,(p)}^-$) and nitric acid vapor ($HNO_{3(g)}$) and result in wet NO_3^- deposition ($NO_{3\,(aq)}^-$). Relative to wet deposition, dry deposition is poorly understood; this is due in part to the complexities of measuring gaseous concentrations and of calculating deposition velocities necessary for quantifying dry deposition rates.

[4] These atmospheric inputs of nitrogen can be a significant source of reactive nitrogen to ecosystems. Nitrogen inputs to the environment, including contributions from the atmosphere and other sources, are a concern worldwide, with potential negative impacts on terrestrial biota, water quality, and human health. Characterizing spatial variability in deposition patterns is a critical research frontier with important implications for improving environmental conditions. Stable isotopes provide a unique means of tracing the fate and transport of atmospheric reactive nitrogen through ecosystems. In this context, we present an initial assessment of the spatial and temporal distribution of the isotopic composition of atmospheric nitrogen deposition, and discuss the utility of this information for tracing sources of nitrogen.

2. Background

[5] Once released to the atmosphere, NO is quickly oxidized via ozone (O_3) to NO_2; this NO_2 is further oxidized via several major chemical reaction pathways. During the daytime, oxygen atoms rapidly exchange between O_3 and NO (reactions (R1) and (R2)) and photolytic production of OH results in oxidation of NO_2 to $HNO_{3(g)}$ via the OH radical (reaction (R3)). This pathway is most prevalent during the summer when concentrations of photochemically produced OH radical are highest [*Calvert et al.*, 1985]. During the nighttime, NO_2 is oxidized by O_3 to produce the NO_3 radical (NO_3) (reaction (R4)), which subsequently combines with NO_2 to form dinitrogen pentoxide (N_2O_5) (reaction (R5)). Hydrolysis of N_2O_5 forms $HNO_{3(g)}$ (reaction (R6)). This pathway is most prevalent during the winter, as N_2O_5 is thermally unstable [*Calvert et al.*, 1985]. Additionally, NO_x can interact with halogen oxides, such as bromine oxide, to form bromine nitrate ($BrONO_2$); this in turn can hydrolyze to NO_3^- [*Morin et al.*, 2008].

$$NO + O_3 \rightarrow NO_2 + O_2 \quad \text{(R1)}$$

$$NO_2 + h\nu \rightarrow NO + O \quad \text{(R2)}$$

$$NO_2 + OH \rightarrow HNO_3 \quad \text{(R3)}$$

$$NO_2 + O_3 \rightarrow NO_3 + O_2 \quad \text{(R4)}$$

$$NO_3 + NO_2 \leftrightarrow N_2O_5 \quad \text{(R5)}$$

$$N_2O_5 + H_2O_{(surface)} \rightarrow 2HNO_3. \quad \text{(R6)}$$

[6] Once formed, HNO_3 can eventually be recycled back to NO_x by photolysis and reaction with OH; this occurs on timescales of several weeks [*Garrett et al.*, 2006]. As a result of this slow recycling rate, HNO_3 is strongly favored in equilibrium between NO_2 and HNO_3 and the removal mechanisms for HNO_3 are considered physical (i.e., dry and wet deposition) rather than chemical [*Garrett et al.*, 2006]. The lifetime of NO_x in the boundary layer is generally less than 2 days, with a longer lifetime expected in the winter (1.2 days) compared to summer (0.27 days) [*Liang et al.*, 1998]. HNO_3 generally has a similar atmospheric lifetime of 1–2 days [*Liang et al.*, 1998]. As a result of these typical lifetimes, NO_x and its oxidation products (NO_y), including HNO_3, are subject to mesoscale transport. For example, 30% of NO_x emitted in the U.S. is exported out of the boundary layer [*Liang et al.*, 1998].

[7] Conservation of the nitrogen atom between NO_x sources and sinks enables $\delta^{15}N$ to be used as a fingerprint of NO_x sources that contribute to atmospheric nitrogen deposition. In particular, NO_x derived from coal combustion is reported to have relatively high $\delta^{15}N$ values, ranging from +5 to +13‰ [*Heaton*, 1987, 1990; *Kiga et al.*, 2000]. $\delta^{15}N$ values for NO_x from vehicle fuel combustion are generally reported to range from +3.7 to +5.7‰ [*Ammann et al.*, 1999; *Moore*, 1977; *Pearson et al.*, 2000], although one study reports negative values (−13 to −2‰) [*Heaton*, 1990]. Natural NO_x sources have lower $\delta^{15}N$ values, including lightning (∼0‰ [*Hoering*, 1957]) and recently measured biogenic soil emissions (−49‰ to −20‰ for NO emitted from fertilized soils [*Li and Wang*, 2008]). As a result of these reported differences in $\delta^{15}N$ values of different NO_x sources, $\delta^{15}N$ can be used to infer NO_x sources that contribute to contemporary nitrate deposition [*Elliott et al.*, 2007; *Freyer*, 1978, 1991; *Hastings et al.*, 2003, 2004; *Heaton*, 1990; *Moore*, 1977; *Wankel et al.*, 2009]; historic nitrogen deposition in ice cores and lake sediments[*Hastings et al.*, 2005; *Wolfe et al.*, 2001, 2003], and nutrient sources to plants [*Ammann et al.*, 1999; *Pearson et al.*, 2000; *Saurer et al.*, 2004].

[8] In comparison, the oxygen isotopic composition of nitrate ($\delta^{18}O$-NO_3^-) is known to be influenced by the relative

contribution of the isotopically enriched $\delta^{18}O$ of O_3 during chemical oxidation reactions [*Hastings et al.*, 2003; *Michalski et al.*, 2003]. The relative proportion of high $\delta^{18}O$ atoms contributed during oxidation is thus used to fingerprint seasonal variations in reaction pathways that are temperature and photochemically sensitive [*Hastings et al.*, 2003; *Jarvis et al.*, 2008; *Michalski et al.*, 2003; *Morin et al.*, 2008; *Savarino et al.*, 2007].

[9] Advances in sample preparation techniques for nitrate isotope analyses, the "microbial denitrifier method" [*Casciotti et al.*, 2002; *Sigman et al.*, 2001] allow high sample throughput of samples characterized by low nitrate concentrations and sample volumes (e.g., precipitation and dry deposition) and thus an improved understanding of nitrate isotope variability across large regions. For example, a recent study demonstrated that the spatial and temporal distribution of nitrate isotopes in wet deposition from 33 National Atmospheric Deposition Program–National Trends Network sites across the northeastern and midwestern U.S. is primarily a function of surrounding stationary source (i.e., electric generating units) emissions [*Elliott et al.*, 2007]. Nitrogen isotopes in wet nitrate deposition ($\delta^{15}N\text{-}NO_3^-{}_{(aq)}$) were determined to be a better predictor of the influence of stationary source emissions than more commonly used "source indicators" including pH, sulfate and nitrate concentrations in precipitation [*Elliott et al.*, 2007]. In this study, we apply the microbial denitrifier method to compare the isotopic composition of dry and wet nitrogen deposition across the high-deposition region of Ohio, Pennsylvania, and New York (U.S.A).

[10] In the U.S., concentrations of dry nitrogen species are measured at over 90 sites across the U.S. by the EPA-funded Clean Air Status and Trends Network (CASTNET). CASTNET measures rural, regionally representative concentrations of dry nitrogen species, including nitric acid vapor ($HNO_{3(g)}$), particulate nitrate ($NO_{3\ (p)}^-$), and particulate ammonium, as well as sulfur dioxide (SO_2) and ozone (O_3) to examine relationships between emissions, air quality, dry deposition, and ecological effects. Weekly cumulative concentrations are measured by drawing air through a three-stage filter pack mounted atop a 10 m tower at a controlled flow rate. CASTNET estimates dry deposition fluxes using an inferential approach wherein the product of deposition velocities (estimated using meteorological measurements and the MultiLayer Model (MLM)) and pollutant concentrations (measured from weekly filter pack samples) is calculated. Since routine measurements of surface exchange rates of gases and particles are still sufficiently complex [e.g., *Wesely and Hicks*, 2000], most dry deposition monitoring programs, including CASTNET, use the inferential approach described above. The spatial distribution of the CASTNET sites in the U.S. is fairly limited; as a result, our understanding of the spatial distribution of dry deposition is less extensive compared to that of wet deposition (there are over 250 sites in the National Atmospheric Deposition Program, National Trends Network).

[11] In addition to active sampling of dry deposition, recent studies have demonstrated the potential to improve our understanding of the spatial distribution of dry nitrogen deposition and gaseous concentrations using passive sampling techniques [*Gilbert et al.*, 2002, 2003; *Golden et al.*, 2008; *Krupa and Legge*, 2000; *Ozden and Dogeroglu*, 2008; *Plaisance et al.*, 2002; *Rabaud et al.*, 2001; *Roadman et al.*, 2003; *Sather et al.*, 2007]. Relative to active sampling techniques, such as those used by the CASTNET program, passive sampling techniques are inexpensive, easy to deploy, and do not require power or other significant infrastructure. As the use of passive samplers has recently increased, it is of particular interest to determine whether passive samplers can also provide an inexpensive collection medium for stable isotope analysis.

[12] In this study, we examine the isotopic composition of dry deposition from 8 CASTNET sites across New York, Pennsylvania, and Ohio (Figure 1 and Table 1) and from passive HNO_3 collectors deployed at a single site in New York. The isotopic composition of dry deposition is compared to simultaneously collected wet deposition from 17 NTN sites across this same region. Total dry deposition (calculated as the sum of HNO_3, $NO_{3\ (p)}^-$, and particulate NH_4^+) across these sites ranges from 0.54 to 3.3 kg N ha^{-1} yr^{-1} and constitutes between 11 and 40% of total deposition by existing NTN and CASTNET protocols (Table 1). The objectives of the study are (1) to document spatial and seasonal variations in the isotopic composition of dry nitrogen deposition from CASTNET sites including $HNO_{3(g)}$ and $NO_{3\ (p)}^-$; (2) examine whether isotopic variations in dry deposition are related to contributions from major NO_x sources (i.e., electric generating units, vehicles) and to what extent dry deposition formation processes and transformations can influence resulting isotopic values in dry deposition; and (3) explore whether HNO_3 for isotopic analysis can be effectively sampled using passive rather than active sampling approaches, which could represent a significant cost saving and allow more detailed spatial sampling.

3. Methods

3.1. Actively Collected Dry Deposition

[13] At each CASTNET site, air is drawn through a three-stage filter pack for a 1 week period at a controlled flow rate to collect gaseous and particulate nitrogen and sulfur species on each filter. The first stage of the filter pack encloses a Teflon® filter that collects SO_4^{2-}, NH_4^+, NO_3^-, Cl^-, and trace elements. The second stage of the filter pack is a nylon filter that collects $HNO_{3(g)}$ and some SO_2. The third stage of the filter pack holds two potassium carbonate impregnated cellulose filters that collect the remaining SO_2. The filter packs are changed weekly each Tuesday and shipped to a centralized analytical chemistry laboratory for analysis where they are stored at 4°C until extraction. Teflon filters containing particulate NO_3^- are extracted in a solution containing bromide, hydrogen peroxide, and sodium hydroxide. Nylon filters containing $HNO_{3(g)}$ are extracted in bromide solution. All eluants are then stored at 4°C.

[14] For isotopic analysis, we collaborated with the CASTNET program to receive weekly $HNO_{3(g)}$ and $NO_{3\ (p)}^-$ filter eluants from 8 sites in Pennsylvania, New York, and Ohio during April 2004 to March 2005 (Figure 1). Excess filter eluant was shipped monthly on ice to the U.S. Geological Survey in Menlo Park, CA where samples were stored at 4°C until isotopic analysis. Weekly sample eluants were pooled into 4 week composites to represent the isotopic composition of $HNO_{3(g)}$ and $NO_{3\ (p)}^-$ over one month periods. The isotopic compositions ($\delta^{15}N$ and $\delta^{18}O$) of $HNO_{3(g)}$ (n = 96,

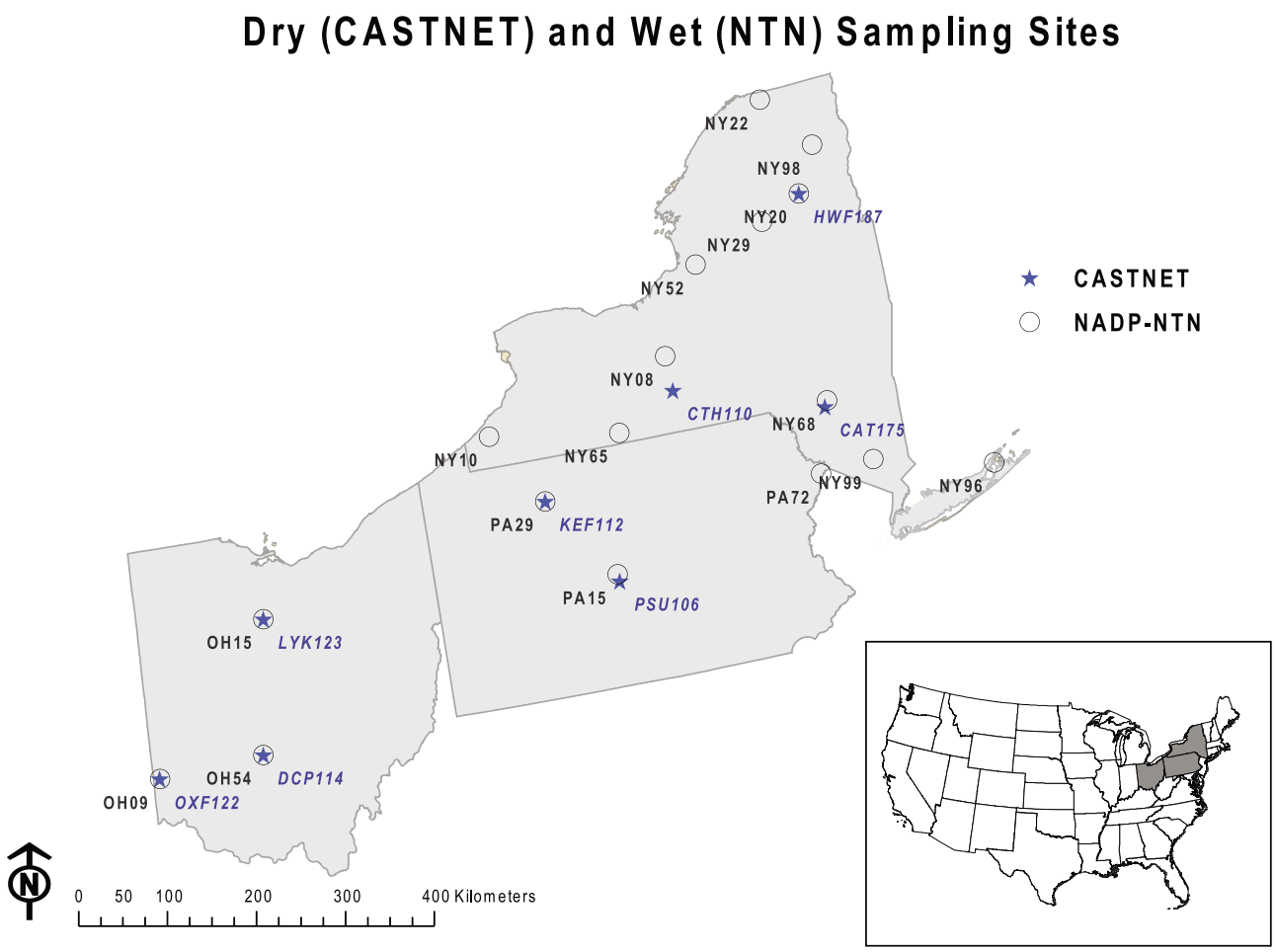

Figure 1. Location of eight CASTNET and 17 NTN sites included in this study.

where n equals the number of sites multiplied by the number of months) and $NO_{3\ (p)}^{-}$ (n = 76, limited instrument time prohibited analysis of all 96 $NO_{3\ (p)}^{-}$ samples) were measured using the microbial denitrifier method described below.

[15] Previous studies have documented that aerosol NO_3^- (i.e., particulate nitrate) sampling can be problematic due to evaporative losses of semivolatile NH_4NO_3 or HNO_3 adsorption [*Ames and Malm*, 2001; *Schaap et al.*, 2004]. For Teflon filters, such as those used in the CASTNET protocol, considerable evaporative losses can result in underestimations of particulate nitrate concentrations [*Ames and Malm*, 2001]. This sampling bias is dependent on temperature and humidity with the highest evaporative losses expected at temperatures exceeding 25°C [*Schaap et al.*, 2004]. We examine the potential source of this sampling bias on our isotopic results in our discussion.

3.2. Wet Deposition

[16] Additionally, we collaborated with the National Atmospheric Deposition Program (NADP)–National Trends Network (NTN) to receive weekly precipitation from 17 NTN sites in New York, Pennsylvania, and Ohio during April 2004–2005 (Figure 1). Six of these 8 sites are colocated within 8 km of CASTNET sites included in this study. These

Table 1. CASTNET Sites Included in This Study and 2004 N Deposition Inputs[a]

CASTNET Site ID	Site Name	Longitude	Latitude	Elevation (m)	$NO_{3\ (aq)}^{-}$ (kg N ha^{-1} yr^{-1})	$HNO_{3(g)}$ (kg N ha^{-1} yr^{-1})	$NO_{3\ (p)}^{-}$ (kg N ha^{-1} yr^{-1})	Total N Deposition[b] (kg N ha^{-1} yr^{-1})
OXF122	Oxford	−84.7286	39.5327	284	2.23	2.09	0.12	6.84
LYK123	Lykens	−83.2605	39.6359	303	3.14	1.97	0.2	8.96
DCP114	Deer Creek	−82.9982	40.9173	267	3.28	2.62	0.12	9.17
KEF112[c]	Kane Experimental Forest	−78.7674	41.5980	622	3.62			
PSU106	Penn State	−77.9319	40.7208	378	3.86	1.56	0.1	8.7
CTH110	Connecticut Hill	−76.6538	42.4006	501	3.04	2.06	0.05	8.72
CAT175[c]	Claryville	−74.5520	41.9422	765				
HWF187	Huntington Wildlife Forest	−74.2232	43.9731	502	2.64	0.42	0.01	4.74

[a]Note that as NH_3 is not monitored at these sites, total N deposition inputs are likely underestimated.
[b]Total deposition = total wet deposition (NO_3^- + NH_4^+) + total dry deposition ($HNO_{3(g)}$ + $NO_{3\ (p)}^{-}$ + $NH_{4\ (p)}^{+}$).
[c]Incomplete dry deposition data during study period.

weekly samples were filtered (0.45 micron Gelman polyethersulfone filter) and NO_3^- concentrations measured by ion chromatography (Dionex DX-500) at the time of initial collection [*National Atmospheric Deposition Program Central Analytical Laboratory*, 2006]. When precipitation volume was sufficient, samples were archived at 4°C at the NADP Central Analytical Laboratory in Champaign, Illinois, USA. Archived weekly samples of wet-only deposition collected during 2004–2005 were pooled into volume-weighted 4 week composite samples to represent monthly deposition, shipped to the U.S. Geological Survey, and analyzed for $\delta^{15}N$ and $\delta^{18}O$ of NO_3^- (n = 204). Samples were continuously stored at 4°C. NO_3^- concentrations show minimal alteration during storage for 3 years; hence, refrigerated, archived samples are suitable for isotopic analysis [*Elliott et al.*, 2007].

3.3. Passive Collection

[17] Passive diffusion samplers for collection of HNO_3 [*Bytnerowicz et al.*, 2005; *Golden et al.*, 2008] were deployed to examine whether passive collectors provide a suitable medium for isotopic analysis. Nine samplers were deployed from 23 April to 20 May 2004 (27 days) at Connecticut Hill (42.4006 latitude, −76.6538 longitude), a CASTNET (CTH110) site in operation since 1987. Samplers were placed at approximately 1.5 m height in triplicate at 3 locations across a 100 m open clearing at the site. Each set of samplers was 12 m apart and each was deployed at the same time. The effectiveness of the passive samplers was tested by: (1) examining whether passive collectors deployed across a gradient at a single site yield replicable results, and (2) determining whether simultaneous collection of passively and actively collected HNO_3 at a single site yield comparable results.

[18] Passive HNO_3 samplers have 47 mm diameter Nylon filters (Nylasorb, Pall Corporation) as the collection medium for HNO_3 and HNO_2. Ambient air passes to the nylon filter through a Zefluor Teflon 47 mm diameter prefilter of 2 μm pore size (Pall Corporation). The filters are housed in a 50 mm polycarbonate Petri dish and are secured by two Teflon rings and one PVC ring. Samplers are protected from wind and rain by a plastic polycarbonate cap. After 27 days, filters were collected and immediately frozen until elution. Samples were eluted in 5 ml of deionized water and placed on an orbital shaker for 30 min. Eluted solutions were frozen until further analysis. From each of the three sampling locations at the Connecticut Hill site, two filter solutions were used for isotopic analysis, the other used for determination of nitrate and nitrite concentrations on a Dionex Ion Chromatograph.

3.4. Isotopic Analysis

[19] For isotopic analysis of wet and dry deposition, the denitrifying bacteria, *Pseudomonas aureofaciens*, were used to convert 20–60 nmoles of NO_3^- into gaseous N_2O prior to isotope analysis [*Casciotti et al.*, 2002; *Sigman et al.*, 2001]. Samples were analyzed for $\delta^{15}N$ and $\delta^{18}O$ in duplicate using a Micromass IsoPrime Continuous Flow Isotope Ratio Mass Spectrometer (use of brand names is for identification purposes only and does not imply endorsement by the U.S. Government) and values are reported in parts per thousand (‰) relative to atmospheric N_2 and Vienna Standard Mean Ocean Water (VSMOW), for $\delta^{15}N$ and $\delta^{18}O$, respectively, using the equation:

$$\delta(\text{in } ‰) = \frac{(R)_{\text{sample}} - (R)_{\text{standard}}}{(R)_{\text{standard}}} \times 1000 \quad (1)$$

where R denotes the ratio of the heavy to light isotope (e.g., $^{15}N/^{14}N$ or $^{18}O/^{16}O$). Samples were corrected using international reference standards USGS 34 ($\delta^{15}N = -1.8‰$; $\delta^{18}O = -27.9‰$), USGS 35 ($\delta^{15}N = +2.7‰$; $\delta^{18}O = +57.5‰$), and N3 ($\delta^{15}N = +4.7‰$; $\delta^{18}O = +25.6‰$) to correct for drift, oxygen isotopic exchange, and blank. Because dry deposition eluant volumes were limited (<20 ml) for isotopic analyses, we were not able to quantify contributions of ^{17}O to the m/z 45 signal of N_2O in this study (see *Hastings et al.* [2003] for further discussion). However, in a separate study, mass-independent contributions of ^{17}O to the m/z 45 signal of N_2O generated from wet nitrate deposition resulted in a mean lowering of $\delta^{15}N$ values by −1.5‰; this correction was determined to slightly dampen seasonal $\delta^{15}N$ differences in wet NO_3^- deposition but did not change spatial $\delta^{15}N$-NO_3^- patterns across the northeastern and midwestern U.S. [*Elliott et al.*, 2007]. In the current study, we consider the influence of ^{17}O to the m/z 45 signal in our discussion of observed $\delta^{15}N$-HNO_3 values relative to those reported for various NO_x sources, but $\delta^{15}N$ values are otherwise reported without correction of contributions of ^{17}O to the m/z 45 signal of N_2O. Additionally, since *Pseudomonas aureofaciens* reduce both nitrate and nitrite to N_2O, the potential interference of nitrite on $\delta^{18}O$-NO_3^- may introduce another analytical artifact [*Casciotti et al.*, 2002, 2007]. Although we do not expect high nitrite concentrations in precipitation or dry deposition eluants, since we did not quantify nitrite concentrations in this study, we cannot rule out the influence of nitrite interferences on our measured $\delta^{18}O$ values. However, in a similar study of dual isotopes of aerosol nitrate, average corrections for nitrite interferences were estimated as +3.3‰ for samples where nitrite concentrations were 3% of total nitrate plus nitrite [*Wankel et al.*, 2009]. Although we observe a large range in $\delta^{18}O$ values in wet and dry nitrate deposition (+45.2‰ to 94.0‰), we expect some error in these values if nitrite is present. Sample replicates had a mean standard deviation (σ) of 0.2‰ for $\delta^{15}N$ (n = 376) and 0.7‰ for $\delta^{18}O$ (n = 376).

3.5. Comparison With Major Emission Sources

[20] To determine whether spatial and temporal patterns in the isotopic composition of dry and wet deposition are associated with the distribution of major NO_x sources, we examined NO_x emissions from the two largest sources in this region, stationary sources (e.g., electric generating units and other industrial facilities) and on road vehicles. Electric utilities and vehicles constitute approximately 1/4 and 1/2, respectively, of total NO_x emissions in the eastern U.S. [*Butler et al.*, 2005]. For stationary sources, we obtained monthly 2004–2005 NO_x emissions data reported to the U.S. EPA from individual facilities. To assess whether spatial and temporal variations in the isotopic composition of dry and wet N are influenced by mobile source NO_x emissions, we compared isotopic values from individual CASTNET and NTN sites with U.S. EPA modeled estimates of monthly, county-level on road vehicle emissions densities (MOBILE

6). Mobile emissions data were not available for the years included in this study (2004–2005), thus we compare 2000 mobile emissions data with 2004–2005 isotopic data. Using ARCINFO (ESRI, Redlands, CA), emission densities from both stationary and vehicle sources were plotted and summed within a 400 km radial area of individual CASTNET and NTN sites using Hawth tools (polygon in polygon analysis). A 400 km radial buffer area was chosen based on previous analysis that indicated the strongest correlations between $\delta^{15}N$ in wet nitrate deposition and stationary sources occurred between 400 and 600 km [*Elliott et al.*, 2007]. To simplify comparisons, monthly emissions data were aggregated into seasonal sums and compared to seasonal average $\delta^{15}N$ and $\delta^{18}O$ values. Relative to anthropogenic emission sources, natural NO_x sources in this high-deposition region are expected to be comparatively minor contributors. The potential contributions from these sources are included in our discussion. Correlations were examined using parametric, linear regressions. All data examined were normally distributed.

4. Results

4.1. Actively Collected Dry Deposition: Seasonal and Spatial Variations in Isotopic Composition

[21] In 96 measurements of $HNO_{3(g)}$, $\delta^{15}N$-$HNO_{3(g)}$ values ranged from −4.9‰ to +10.8‰, with a mean value of +3.2‰. $\delta^{18}O$-$HNO_{3(g)}$ values ranged from +51.6‰ to +94.0‰, with a mean value of +77.4‰ (n = 95). Both $\delta^{15}N$ and $\delta^{18}O$ of $HNO_{3(g)}$ are normally distributed. In $HNO_{3(g)}$, mean NO_3^- concentrations in filter eluant were 16.9 μM.

[22] In comparison, we observed larger ranges of $\delta^{15}N$ and $\delta^{18}O$ values in $NO_{3(p)}$ than in $HNO_{3(g)}$. $\delta^{15}N$-$NO_{3(p)}$ values ranged from −9.5‰ to +14.1‰, with a mean value of +6.8‰ (n = 76), and $\delta^{18}O$-$NO_{3(p)}$ values ranged from +45.2‰ to +92.7‰, with a mean value of +75.2‰ (n = 76). The mean NO_3^- concentration in $NO_{3(p)}$ filter eluant was 12.6 μM.

[23] Seasonal patterns in both $\delta^{15}N$ and $\delta^{18}O$ of $HNO_{3(g)}$ and $NO_{3(p)}$ are distinct and consistent across all sites (Figure 2), but with a slightly higher amplitude for the $NO_{3\ (p)}^-$. Mean $\delta^{15}N$ values are 6.2‰ and 7.6‰ higher in winter (December–February) than in summer (June–August) for $HNO_{3(g)}$ and $NO_{3(p)}$, respectively. Similarly, mean $\delta^{18}O$ values are 15.4‰ and 22.3‰ higher in the winter than in summer for $HNO_{3(g)}$ and $NO_{3(p)}$, respectively (Figure 2). Mean $NO_{3\ (p)}^-$ filter eluant concentrations were nearly an order of magnitude higher in the winter (26.3 μM) than in the summer (3.0 μM). In contrast, mean $HNO_{3(g)}$ concentrations in filter eluant were less seasonally variable, with mean winter $HNO_{3(g)}$ concentrations (19.8 μM) similar to mean summer concentrations (18.4 μM) (Figure 2).

[24] $\delta^{15}N$-$HNO_{3(g)}$ and $\delta^{15}N$-$NO_{3\ (p)}^-$ values are higher at the western sites and lower at the eastern sites during all seasons (Figure 3). In particular, the highest $\delta^{15}N$-$HNO_{3(g)}$ and $\delta^{15}N$-$NO_{3\ (p)}^-$ values occur at sites in Ohio and Pennsylvania during the winter, with notably lower $\delta^{15}N$-$HNO_{3(g)}$ further east (Figure 3). The spatial gradient in $\delta^{15}N$-$HNO_{3(g)}$ and $\delta^{15}N$- $NO_{3\ (p)}^-$ persists throughout all seasons; however, it is least pronounced during summer. In comparison, $\delta^{18}O$-$HNO_{3(g)}$ and $\delta^{18}O$- $NO_{3\ (p)}^-$ values during winter are fairly consistent across 7 of the 8 sites, with the exception of a single site (HWF) where we observe notably lower $\delta^{18}O$-$HNO_{3(g)}$ and $\delta^{18}O$-$NO_{3\ (p)}^-$ values (Figure 4).

4.2. Comparison of the Isotopic Composition of Wet and Dry N Deposition

[25] $\delta^{15}N$ and $\delta^{18}O$ values of NO_3^- in wet deposition from 17 NTN sites exhibit similar spatial and temporal patterns to those of dry NO_3^- deposition. $\delta^{15}N$ values are generally lowest at the most northeastern sites throughout the seasons (Figure 3). Seasonal variations in both $\delta^{15}N$ and $\delta^{18}O$ values in wet NO_3^- deposition are also pronounced (Figure 2), with the highest values in winter and lowest values in summer.

[26] The higher $\delta^{15}N$ values we observed in dry deposition compared to wet deposition have been reported elsewhere [e.g., *Freyer*, 1991; *Garten*, 1996]. $\delta^{15}N$-$HNO_{3(g)}$ values are an average of 3.4‰ higher than corresponding $\delta^{15}N$-$NO_{3\ (aq)}^-$ values from colocated sites. The average difference is higher during the winter (4.6‰) and fall (4.1‰) than in the spring (2.8‰) and summer (2.1‰). In comparison, $\delta^{15}N$-$NO_{3\ (p)}^-$ values are an average of 6.7‰ higher than corresponding $\delta^{15}N$-$NO_{3\ (aq)}^-$ values from colocated sites. This difference is higher during the winter (8.0‰), spring (6.0‰), and fall (6.9‰) than in the summer (4.4‰).

4.3. Passively Collected Dry Deposition

[27] Replicate HNO_3 passive samplers (n = 6), deployed at three sites simultaneously at Connecticut Hill, yielded similar isotopic values (Table 2). Within each set of paired samplers, the standard deviations for replicate pairs ranged from 0 to 0.3‰ for $\delta^{15}N$ and from 0.3 to 1.0‰ for $\delta^{18}O$. Additionally, the spatial variation in samplers deployed across the 100 m opening at Connecticut Hill yielded similar isotopic values. $\delta^{15}N$ values ranged from −1.4 to −1.0‰ (n = 6) whereas $\delta^{18}O$ values ranged from +69.3 to +70.8‰ (n = 6). Across these three sites, the standard deviation of isotopic values is 0.0‰ and 0.4‰ for $\delta^{15}N$ and $\delta^{18}O$, respectively.

[28] In addition to examining replication of the passive samplers across the CASTNET site, we also compared $\delta^{15}N$ and $\delta^{18}O$ values of HNO_3 collected during a similar time period using passive and active collection methods. The CASTNET sample, representing May 2004, was characterized by −0.6 and +76.5‰ for $\delta^{15}N$-HNO_3 and $\delta^{18}O$-HNO_3, respectively. The mean of passively collected samples (23 April to 20 May 2004, n = 6) was −1.2 and +70.2‰ for $\delta^{15}N$-HNO_3 and $\delta^{18}O$-HNO_3, respectively. The results indicate lower $\delta^{15}N$ and $\delta^{18}O$ values for the passively collected samples (−0.6‰ for $\delta^{15}N$ and −6.4 for $\delta^{18}O$).

5. Discussion

[29] Two factors can influence the spatial and temporal distribution of isotopes in wet and dry deposition across this region: (1) retention of seasonal and spatial variations in NO_x source signatures by resulting dry deposition, and (2) seasonal and spatial variations in oxidation chemistry, formation processes, and equilibrium reactions across the region. In the following sections, we address these two factors, as well as results from a pilot study to explore the potential efficacy of passive collectors as a medium for isotopic analysis.

5.1. NO_x Source Contributions to Dry Deposition

[30] Table 3 summarizes the correlation coefficients and significance levels for linear regressions between $\delta^{15}N$, $\delta^{18}O$, and nitrate concentrations and fossil fuel NO_x emissions within 400 km of CASTNET and NTN sites (Figures 5

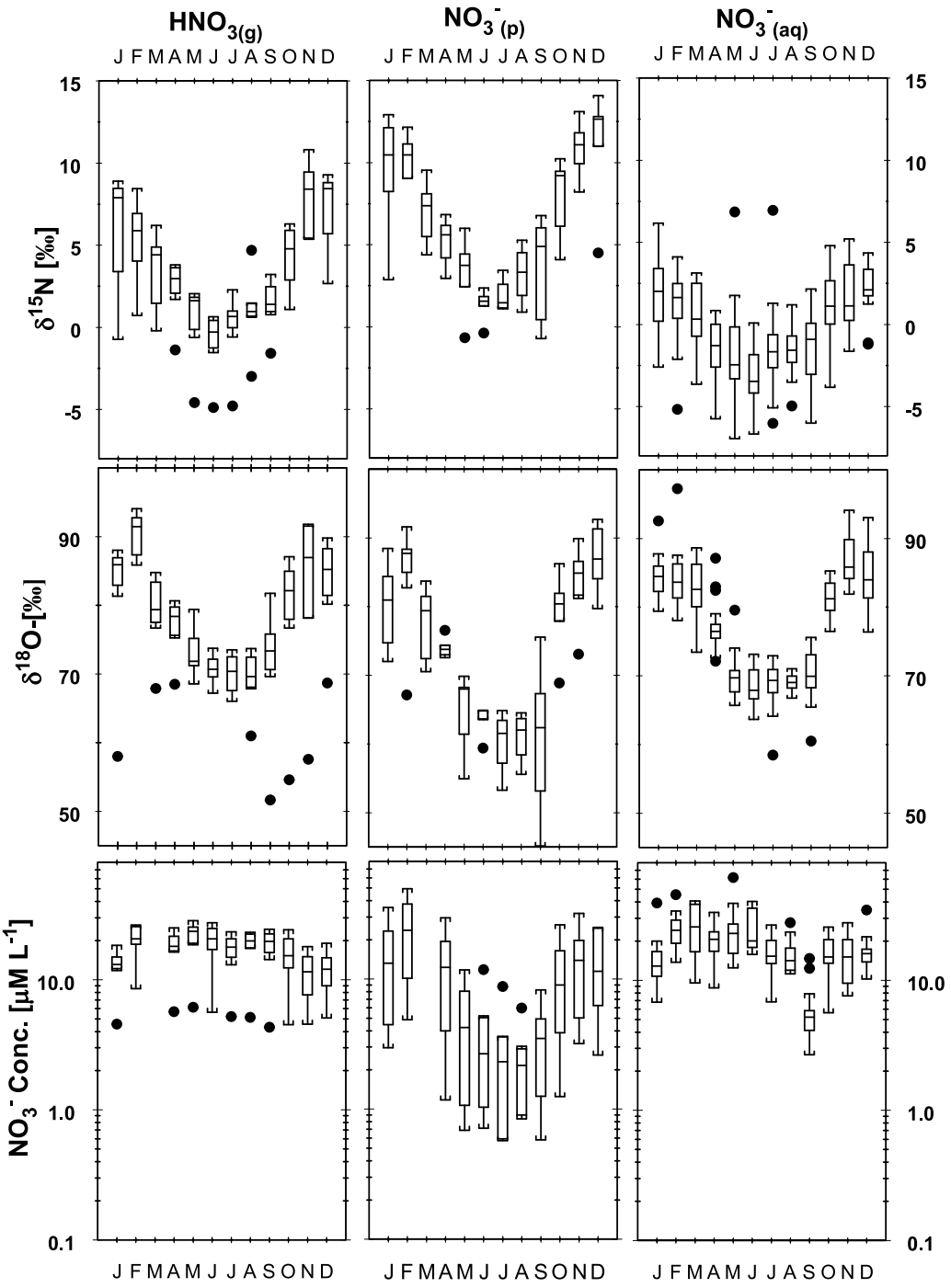

Figure 2. Temporal variations in $\delta^{15}N$, $\delta^{18}O$, and nitrate concentrations in dry and wet deposition from eight CASTNET and 17 NTN sites in New York, Pennsylvania, and Ohio. The rectangular boxes indicate the interquartile range (first and third quartiles); median values are indicated by the centerline within each box; values within 1.5 times the interquartile range are indicated by "whiskers"; outliers are indicated by circles.

and 6). We find no strong evidence that $\delta^{18}O\text{-}NO_3^-$ retains a NO_x source signature (Table 3 and Figure 7); these findings agree with previous studies indicating $\delta^{18}O\text{-}NO_3^-$ values are primarily controlled by the proportion of O_3 atoms incorporated during oxidation to HNO_3 [*Hastings et al.*, 2003; *Jarvis et al.*, 2008; *Michalski et al.*, 2003; *Morin et al.*, 2008; *Savarino et al.*, 2007]. In addition to fossil fuel combustion sources, other potential sources of NO_x to this region include lightning, biomass burning, and biogenic soil emissions. Constraining the relative magnitude of these inputs to our study region is difficult given spatio-temporal variability in these sources. However, recent work using satellite observations [e.g., *Jaegle et al.*, 2005] and aircraft measurements [e.g., *Hudman et al.*, 2007] suggest that "bottom-up" estimates of NO_x emissions from natural sources may be significantly underestimated. Nonetheless, given the magni-

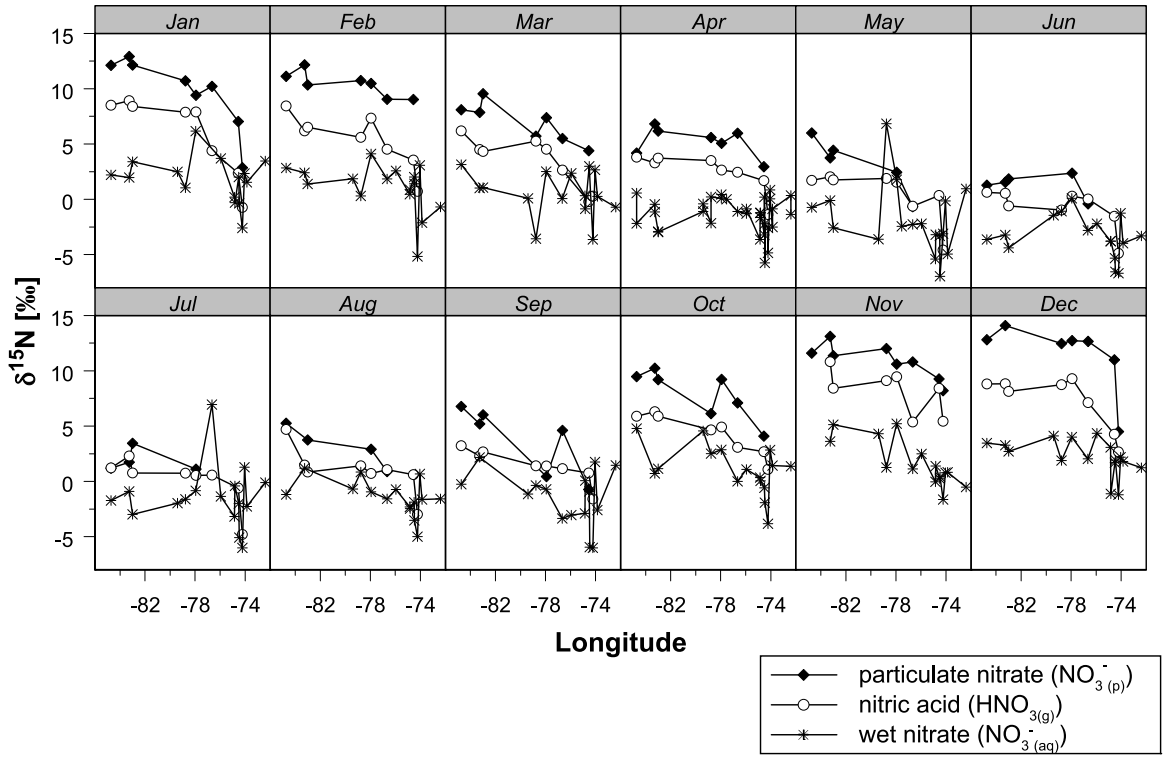

Figure 3. Spatial distribution of monthly δ^{15}N-$HNO_{3(g)}$, δ^{15}N-$NO_{3(p)}$, and δ^{15}N- $NO_{3\,(aq)}^{-}$ values from west to east.

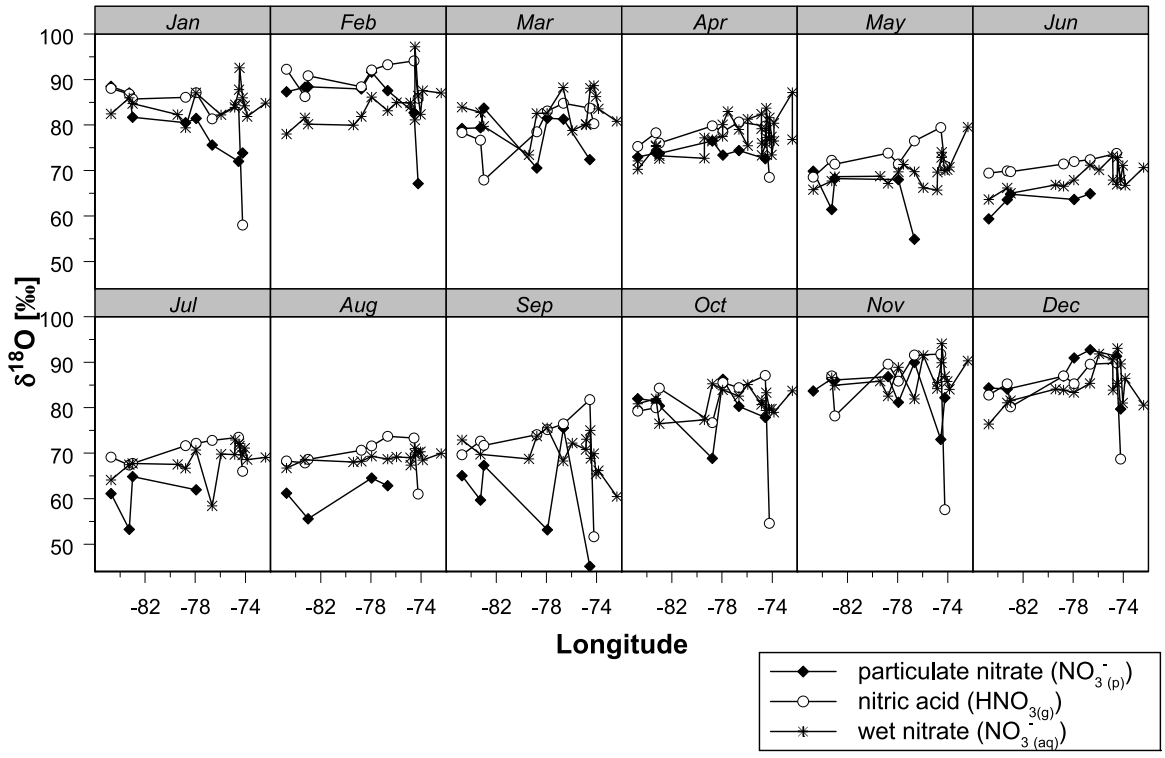

Figure 4. Spatial distribution of monthly δ^{18}O-$HNO_{3(g)}$, δ^{18}O-$NO_{3(p)}$, and δ^{18}O- $NO_{3\,(aq)}^{-}$ values from west to east.

Table 2. Reproducibility of HNO_3 Isotopic Composition Sampled Using Passive HNO_3 Collectors Located at Three Sites Across a 100 m Clearing and Comparison With Actively Collected HNO_3 at the Colocated CASTNET Site

Station	$\delta^{15}N$ (‰)	$\delta^{18}O$ (‰)	Mean $\delta^{15}N$ (‰)	Mean $\delta^{18}O$ (‰)	Standard Deviation ($\delta^{15}N$) (‰)	Standard Deviation ($\delta^{18}O$) (‰)
A	−1.3	69.7	−1.3	69.9	0.0	0.3
A	−1.2	70.1				
B	−1.2	70.8	−1.2	70.6	0.0	0.3
B	−1.2	70.4				
C	−1.4	70.7	−1.2	70.0	0.3	1.0
C	−1.0	69.3				
Monthly HNO_3 composite at CASTNET site (CTH 110)	−0.6	76.5				

tude of fossil fuel NO_x emissions in the Ohio, New York, and Pennsylvania region, the influence of these natural emission sources is expected to be comparatively minor. For example, although soil NO_x emissions are estimated to be 22% of the global NO_x budget, they are most significant from fertilized agricultural soils in the midlatitudes and seasonally dry tropical ecosystems [*Jaegle et al.*, 2005]. Moreover, soil emissions and lightning-generated NO_x are expected to be seasonally variable, with the highest contributions during the warmer months when thunderstorms are more frequent and soil microbial activity is more intense.

[31] The strongest and most consistent correlations are observed between $\delta^{15}N$-HNO_3 and stationary source NO_x emissions ($0.64 < r^2 < 0.92$) (Figure 5 and Table 3). Concentrations of HNO_3 are also correlated with stationary source emissions, suggesting that the spatial distribution of stationary sources is a primary control on HNO_3 formation and associated $\delta^{15}N$-HNO_3 values (Table 3). The strong correlations observed in winter may result from lower mixing heights and longer NO_x lifetimes observed in winter. These conditions should aid the efficient transport of stationary source NO_x and resulting HNO_3, to downwind CASTNET sites. In comparison, the weaker summer correlations may result from increased NO_x contributions from soils and lightning, dilution of NO_x and HNO_3 with a higher mixing height, and HNO_3 formation via decomposition of hydroxy organic nitrates (such decomposition can comprise up to 30% of HNO_3 formation during summer in the U.S. [*Liang et al.*, 1998]). Given the lifetimes of NO_x and HNO_3, it is likely that the unexplained variance in the correlations reported in Table 3 can be partially attributable to NO_x sources beyond the 400 km used in these analyses.

[32] Significant correlations are also observed between $\delta^{15}N$-$NO_3^-{}_{(p)}$ fractions and stationary source emissions during the winter and spring (Figure 5 and Table 3). Limited summer samples of $NO_3^-{}_{(p)}$ ($n = 5$) inhibit statistically significant correlations between $\delta^{15}N$ and emissions. Concentrations of particulate nitrate are correlated with emissions, except during the summer, suggesting that particulate nitrate formation results from stationary source emissions (Table 3). Since $NO_3^-{}_{(p)}$ formation is favored at lower temperatures, low $NO_3^-{}_{(p)}$ concentrations during warmer months may influence resulting $\delta^{15}N$-$NO_3^-{}_{(p)}$ values and thus correlations with stationary source NO_x emissions.

[33] The strong correlations we observe between $\delta^{15}N$ of dry deposition and stationary source NO_x emissions are similar to that recently reported for $\delta^{15}N$ of wet NO_3^- deposition [*Elliott et al.*, 2007]. Although isotope fractionations occur between $HNO_{3(g)}$, $NO_3^-{}_{(p)}$, and $NO_3^-{}_{(aq)}$ (e.g., the offset $\delta^{15}N$ values between wet and dry NO_3^- fractions), $\delta^{15}N$ values are still strongly correlated with NO_x emissions. This further indicates that although fractionations likely occur between N species, they do not impede the use of $\delta^{15}N$ values as indicators of contributions of stationary sources to wet [*Elliott et al.*, 2007], and now dry deposition.

[34] In comparison to dry deposition, $\delta^{15}N$ in wet nitrate deposition is not as strongly influenced by stationary source NO_x emissions in this study (Figure 5 and Table 3). This is in contrast to the strong correlations ($0.67 < r^2 < 0.78$, $p < 0.001$) previously reported between stationary source emissions and $\delta^{15}N$ in wet nitrate deposition for 33 sites spanning from Ohio to Maine [*Elliott et al.*, 2007]. One potential explanation for this difference is that the earlier study spanned the entire deposition gradient rather than the sites in these three states with high-deposition loads. As a result, the emission densities included in the present study span a smaller range than those included in the previous study.

[35] In comparison with stationary source emissions, we observed no consistent significant correlations between $\delta^{15}N$, $\delta^{18}O$, or nitrate concentrations in dry or wet deposition and mobile NO_x emissions (Table 3). Although occasional correlations were observed during the spring and summer (Table 3), the fact that these correlations are not consistent across seasons suggests that vehicle NO_x emissions are not a dominant factor in the isotopic composition of dry deposi-

Table 3. Correlation Coefficients and Significance Levels for Regressions Between $\delta^{15}N$, $\delta^{18}O$, and Nitrate Concentrations of Wet and Dry Deposition With Stationary and Vehicle NO_x Emissions Within 400 km of CASTNET and NTN Sites[a]

	Constituent	Winter	Spring	Summer	Fall
		Stationary NO_x Emissions			
$HNO_{3(g)}$	$\delta^{15}N$	0.92***	0.89***	0.64*	0.76**
	$\delta^{18}O$				
	$[NO_3^-]$		0.59*	0.75**	0.60*
$NO_3^-{}_{(p)}$	$\delta^{15}N$	0.62*	0.89**		
	$\delta^{18}O$	0.69*			
	$[NO_3^-]$	0.78**	0.54***		0.61*
$NO_3^-{}_{(aq)}$	$\delta^{15}N$		0.26*		0.61***
	$\delta^{18}O$	0.52**	0.40**	0.38*	
	$[NO_3^-]$				
		On Road NO_x Emissions			
$HNO_{3(g)}$	$\delta^{15}N$				
	$\delta^{18}O$		0.60*	0.51*	
	$[NO_3^-]$				
$NO_3^-{}_{(p)}$	$\delta^{15}N$		0.66*		
	$\delta^{18}O$			0.88*	
	$[NO_3^-]$		0.58*		
$NO_3^-{}_{(aq)}$	$\delta^{15}N$		0.23*		
	$\delta^{18}O$				
	$[NO_3^-]$			0.25*	

[a]Significance levels (p values) are indicated as follows: <0.001 by ***, <0.01 by **, and <0.05 by *.

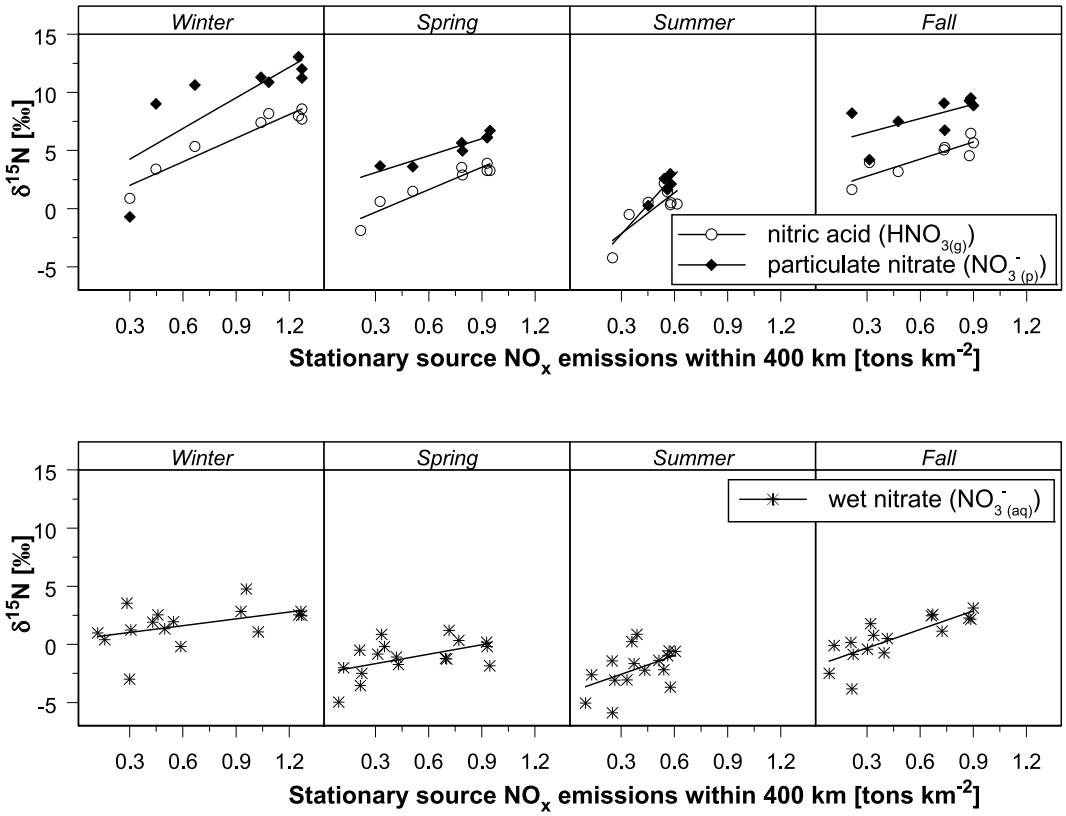

Figure 5. Correlations between (top) δ^{15}N-$HNO_{3(g)}$, δ^{15}N-$NO_{3(p)}$ and (bottom) δ^{15}N-$NO_{3\ (aq)}^{-}$ and stationary source NO_x emissions within 400 km radial area of study sites. Significant correlations are indicated by a linear regression trend. Correlation coefficients and significance levels are shown in Table 3.

tion, wet deposition, or nitrate concentrations at these study sites.

[36] The lack of consistent correlations may arise from contrasting temporal windows in vehicle emissions estimates and isotope data, from poor estimates of actual vehicle emissions by MOBILE 6 [*NARSTO*, 2005], or from uncertainty in the isotopic composition of vehicle NO_x emissions. However, these results may also indicate that vehicle NO_x emissions are not transported as far as those from stationary sources, and thus have little influence at CASTNET sites that are intentionally established in locations far from urban centers and highways. We note that examining the isotopic composition of vehicular emissions and their fate in the environment is a critical area for future research with important implications for landscape biogeochemistry.

[37] In general, stationary source NO_x emissions are highest in the winter months during peak heating demand. As a result, mean NO_x emission densities in the winter are nearly double those in the summer (0.16 and 0.09 tons km^{-2} in the winter and summer, respectively). Although emission densities in summer are nearly half those in winter, air conditioning demand frequently creates a local maxima during summer. Additionally, natural NO_x sources, including lightning and biogenic NO_x emitted during soil nitrification and denitrification contribute more during summer; these sources are characterized by low δ^{15}N values relative to fossil fuel sources. For the eight sites included in this study, temporal patterns of δ^{15}N-$HNO_{3(g)}$ and NO_x emissions are strongly correlated for most sites (Figure 6). We observe the strongest correlations between δ^{15}N-$HNO_{3(g)}$ and NO_x emissions at KEF112 ($r^2 = 0.74$, $p < 0.001$) and LYK123 ($r^2 = 0.76$, $p < 0.001$). We also observe strong correlations on a site by site basis at other sites, including CTH110 ($r^2 = 0.57$, $p < 0.005$), DCP114 ($r^2 = 0.64$, $p < 0.005$), OXF122 ($r^2 = 0.68$, $p < 0.005$) and PSU106 ($r^2 = 0.62$, $p < 0.005$). The strength of these correlations seems to be independent of NO_x emission densities, as the highest emission densities occur at the Ohio sites (OXF122, LYK123, DCP114). Correlations at the most remote sites (also located furthest east), CAT175 and HWF187, are not significant, suggesting the influence of other emission sources at these sites, or that additional fractionations during transport are masking the emission source signature. Correlations between δ^{15}N-$NO_{3(p)}$ and NO_x emissions density are similar to those observed with δ^{15}N-$HNO_{3(g)}$ for sites where complete temporal data are available (Figure 6). However, for sites with missing δ^{15}N-$NO_{3(p)}$ data, the correlations are not significant (CAT175, HWF187, and KEF112). The strong correlations illustrated in Figure 6 suggest that the temporal variations in δ^{15}N-$HNO_{3(g)}$ are directly linked to stationary NO_x emissions. For example, OXF 122 follows the expected pattern of highest NO_x emissions during December–January, with a secondary peak in July. δ^{15}N-$HNO_{3(g)}$ values follow this pattern remarkably well. As another example, peak NO_x emissions occur much earlier at the LYK123 site (October and November), and the highest δ^{15}N-$HNO_{3(g)}$ values also occur during this time period at this site.

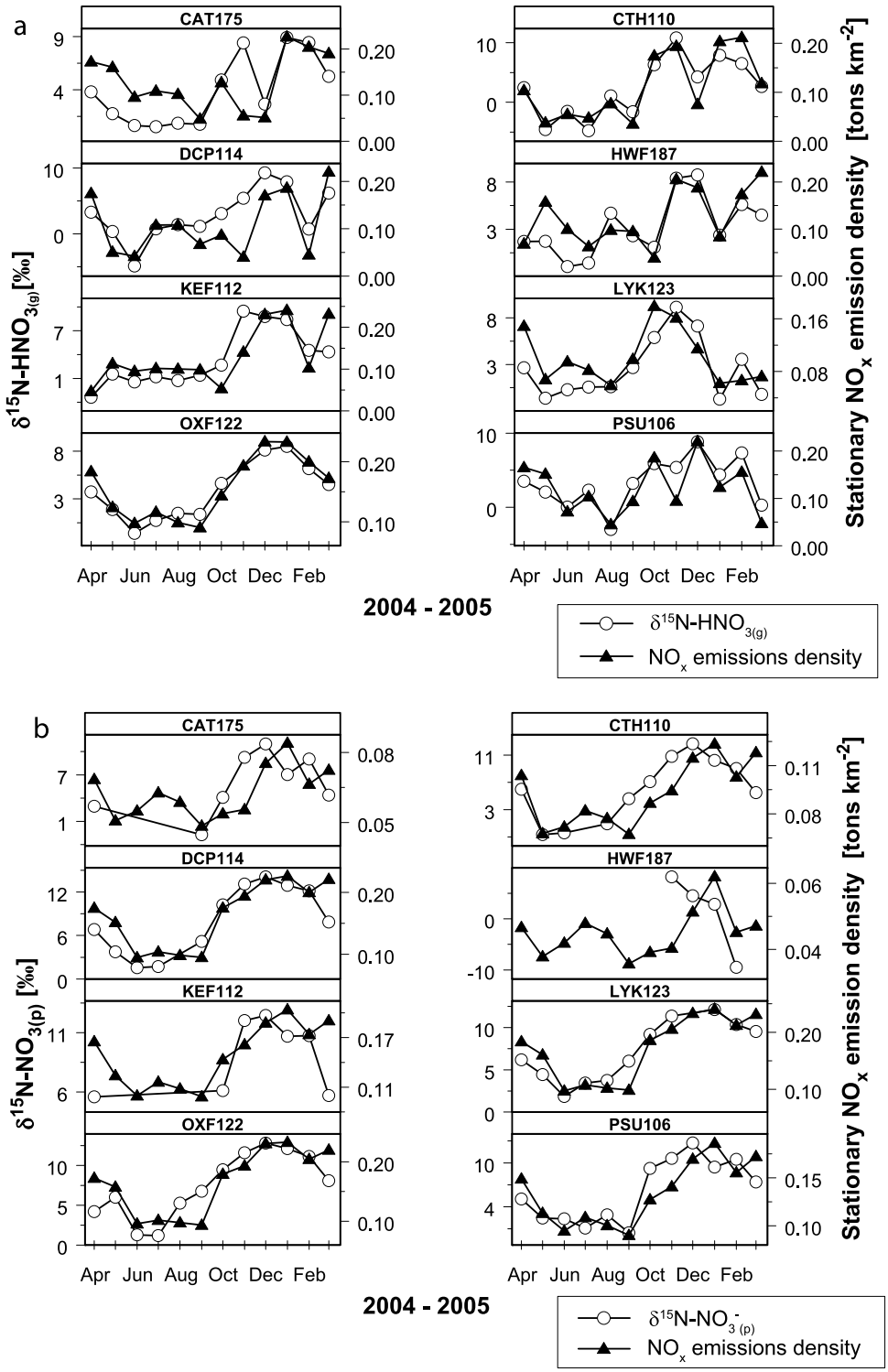

Figure 6. (a) Temporal variations in δ^{15}N-HNO$_{3(g)}$ (left *y* axis) and NO$_x$ emissions density (right *y* axis) from surrounding (400 km radial area) stationary sources. (b) Temporal variations in δ^{15}N-NO$_{3(p)}$ (left *y* axis) and NO$_x$ emissions density (right *y* axis) from surrounding (400 km radial area) stationary sources.

5.2. Atmospheric Oxidation Reactions, Formation Processes, and Isotopic Values

[38] Various atmospheric processes can influence isotopic values of atmospheric N species including: (1) seasonality of oxidation pathways, (2) fractionations, (3) partitioning between wet and dry components, (4) spatial gradients in climate, and (5) spatial gradients in atmospheric chemistry.

[39] Seasonality in the chemical oxidation pathways (reactions (R1)–(R6)) is a major determinant of δ^{18}O-NO_3^- values [*Hastings et al.*, 2003; *Michalski et al.*, 2003] due to high

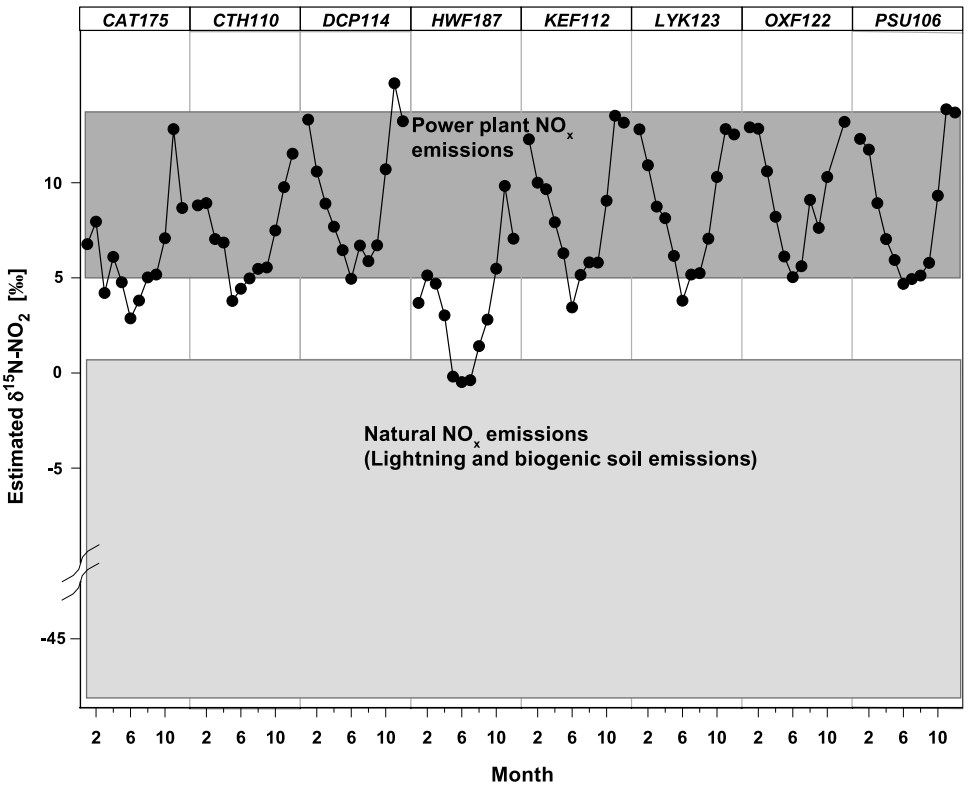

Figure 7. Estimated δ^{15}N-NO_2 values for CASTNET sites based on kinetic isotopic fractionation between NO_2 and HNO_3 [*Freyer*, 1991] and contributions of ^{17}O to the m/z 45 signal of N_2O. Shaded boxes represent reported ranges in the literature for major NO_x sources including power plant NO_x emissions [*Heaton*, 1987; *Kiga et al.*, 2000] and natural sources including NO_x generated from electrical discharges (i.e., lightning) [*Hoering*, 1957] and biogenic NO emissions from fertilized soils [*Li and Wang*, 2008].

δ^{18}O values contributed by O_3 (+90 to +120‰) [*Johnston and Thiemens*, 1997; *Krankowsky et al.*, 1995] to nitrate formation [*Hastings et al.*, 2003]. This chemical fingerprinting of δ^{18}O- NO_3^- by O_3 has since been used to characterize the predominance of multiple chemical pathways [*Jarvis et al.*, 2008; *Morin et al.*, 2008; *Savarino et al.*, 2007]. The seasonality in these channels is a function of both temperature (N_2O_5 thermally decomposes) and solar radiation (OH is photolytically produced). Hence, as expected, the combined effects of temperature and solar radiation control δ^{18}O values in $NO_{3\,(p)}^-$ and $NO_{3\,(aq)}^-$ (Table 4). While the effects of temperature and solar radiation also influence δ^{15}N values in dry and wet deposition (Table 4), these correlations are less significant than those for δ^{18}O and are also less significant than with stationary source emissions. These findings contrast with those from the Arctic, where temperature was determined to be a major driver of δ^{15}N-NO_3^- values in all seasons except spring when snowpack emissions are maximal [*Morin et al.*, 2008].

[40] The seasonality of oxidation pathways in reactions (R1)–(R6) can also fractionate ^{15}N and ^{18}O in wet and dry deposition. For example, the winter dominance of the N_2O_5 channel (reactions (R4)–(R6)) can result in equilibrium fractionations causing higher δ^{15}N values in more oxidized species [*Freyer et al.*, 1993]. Additionally, in highly polluted atmospheres where NO_x concentrations exceed O_3 concentrations, equilibrium reactions between NO and NO_2 can cause a large equilibrium isotope effect (α = 1.028) [*Freyer et al.*, 1993]. This equilibrium fractionation can cause higher winter δ^{15}N-NO_2 values and lower summer δ^{15}N-NO_2 values, although subsequent studies have ruled out equilibrium fractionations as a control on seasonal δ^{15}N variability in relatively pristine Bermuda and Arctic environments [*Hastings et al.*, 2003, 2004; *Jarvis et al.*, 2008]. Since NO and NO_2 concentrations are not monitored at CASTNET sites, this equilibrium fractionation remains a potential influence on the seasonality we observe. For example, in higher-emission areas of Ohio and western Pennsylvania, equilibrium reac-

Table 4. Correlation Coefficients and Significance Levels for δ^{15}N and δ^{18}O of Dry and Wet NO_3^- Deposition With Mean Monthly Temperature and Solar Radiation Measurements From Individual CASTNET Sites[a]

	Constituent	Temperature	Solar Radiation	Temperature Plus Solar Radiation
$HNO_{3(g)}$	δ^{15}N	0.25***	0.44***	0.43***
	δ^{18}O	0.29***	0.27***	0.38**
$NO_{3\,(p)}^-$	δ^{15}N	0.19***	0.38***	0.44**
	δ^{18}O	0.47***	0.59***	0.70***
$NO_{3\,(aq)}^-$	δ^{15}N	0.09**	0.16***	0.26*
	δ^{18}O	0.77***	0.71***	0.88***

[a]Meteorological data were collected on an hourly basis. Correlation coefficients and significance levels for the combined effects of temperature and solar radiation are shown in the last column. Significance levels (p values) are indicated as follows: <0.001 by ***, <0.01 by **, and <0.05 by *.

tions between NO-NO_2 may be partially responsible for the "source" signature we observe in $\delta^{15}N$ of dry and wet nitrate deposition.

[41] The oxidation of NO_2 to $HNO_{3(g)}$ in reaction (R3) can result in a fractionation of 0.9971 [*Freyer*, 1991], thus resulting in $\delta^{15}N$-$HNO_{3(g)}$ values approximately 3‰ lower than $\delta^{15}N$-NO_2. As our observed values of $\delta^{15}N$ in wet and dry $HNO_{3(g)}$ deposition are lower than most reported $\delta^{15}N$ values for NO_x sources, we can estimate $\delta^{15}N$-NO_2 values that led to HNO_3 formation. Based on the fractionation reported by *Freyer* [1991], as well as potential contributions of $\Delta^{17}O$ to m/z 45 signal of HNO_3 (assumed to result in a net lowering of $\delta^{15}N$ by 1.5‰), we estimate $\delta^{15}N$-NO_2 using the following equation:

$$\delta^{15}N - NO_2 = \left(\delta^{15}N - HNO_3 + \left(1000^*(1 - 0.9971)\right)\right) + 1.5 \quad (2)$$

The resulting $\delta^{15}N$-NO_2 values range from −0.5 to +15‰ and are shown in Figure 7 for individual CASTNET sites. These estimated $\delta^{15}N$-NO_2 values fall more closely within the range of reported values for NO_x sources that are expected to influence these sites, mainly NO_x derived from electricity generation and natural NO_x sources (lightning and biogenic soil emissions) (Figure 7). It is assumed that vehicle NO_x contributions to these sites are not significant given the location of CASTNET sites away from urban areas and major vehicular sources, and the lack of correlations we observe between $\delta^{15}N$ and vehicle NO_x emissions. As suggested by Figure 7, these CASTNET sites receive a mixture of NO_x from both power plant and natural NO_x sources that is highly seasonal. However, until more precise characterization of ^{15}N source values and isotope fractionations during subsequent oxidation reactions is completed, a more precise partitioning of source contributions is not possible.

[42] The partitioning between $NO_{3\ (p)}^-$ and HNO_3 is dependent on temperature, relative humidity, and NH_3 concentrations. Solid phase NH_4NO_3 is formed when relative humidity is lower than the deliquescence relative humidity, whereas HNO_3 and NH_3 dissolve into the aqueous phase when the relative humidity exceeds the deliquescence relative humidity [*Ansari and Pandis*, 2000; *Morino et al.*, 2006] (reactions (R7) and (R8)).

$$(R7) \qquad NH_4NO_{3(s)} \leftrightarrow HNO_{3(g)} + NH_{3(g)}$$

$$(R8) \qquad HNO_{3(g)} + NH_{3(g)} \leftrightarrow NO_{3(aq)}^- + NH_{4(aq)}^+.$$

It is expected that the dynamic equilibrium in reaction (R7) will affect the isotopic composition of $HNO_{3(g)}$ and $NO_{3\ (p)}^-$. The partitioning between gas and solid phase should shunt the isotopically lighter fraction into the gas phase. This process likely contributes to the consistent offset observed between $\delta^{15}N$-HNO_3 and $\delta^{15}N$-$NO_{3\ (p)}^-$.

[43] Climatic gradients across the study region, including temperature and solar radiation, may influence the relative importance of each oxidation pathway to individual CASTNET sites. Based on hourly temperature and solar radiation measurements from individual CASTNET sites, mean temperatures and solar radiation are highest at the most western sites and decrease toward the northeast. Given the fractionations and relative favorability of contrasting oxidation channels, we expect higher $\delta^{15}N$ and $\delta^{18}O$ values at eastern sites. However, the opposite spatial trends in $\delta^{15}N$ are observed (Figure 3), further suggesting that the primary control on $\delta^{15}N$ spatial variability is the influence of stationary source NO_x emissions. In comparison, $\delta^{18}O$ values in dry and wet deposition often increase in an easterly direction, with the exception of the easternmost site (HWF187) where consistently low $\delta^{18}O$ values are observed (Figure 4). This pattern in $\delta^{18}O$-NO_3^- values indicates that climatic gradients indeed influence the spatial distribution of $\delta^{18}O$ values observed in dry and wet deposition.

[44] In addition to the influence of temperature and solar radiation on oxidation pathways, other chemical gradients may influence $\delta^{18}O$ values. For example, higher sulfate aerosol concentrations in Ohio and western Pennsylvania result in a spatial gradient in N_2O_5 lifetimes across the midwestern and northeastern U.S. [*Brown et al.*, 2006]. In particular, higher sulfate concentrations cause faster hydrolysis of N_2O_5 in Ohio and western Pennsylvania than in states further east. The longer N_2O_5 lifetimes observed at eastern sites may also cause the higher $\delta^{18}O$ values observed in wet and dry NO_3^- deposition at more northeastern sites. We observe the strongest $\delta^{18}O$-NO_3^- gradients during the summer, when sulfate concentrations are generally highest, and when N_2O_5 lifetime differences would be most important.

[45] Under certain atmospheric conditions, ammonium nitrate (NH_4NO_3) can volatilize from Teflon® filters packs during the weekly CASTNET sampling period, dissociating to form NH_3 and HNO_3 [*Ames and Malm*, 2001]. This causes overestimated $HNO_{3(g)}$ concentrations and underestimated $NO_{3(part)}^-$ concentrations. Although this sampling bias has been documented [e.g., *Ames and Malm*, 2001; *Schaap et al.*, 2004, and references therein], the magnitude, geographic extent and seasonal variations are not well documented.

[46] Here we consider the potential for these artifacts to influence $\delta^{15}N$ and $\delta^{18}O$ values in dry nitrate deposition. If the dissociation of NH_4NO_3 on the filter surface causes a large fractionation between either $HNO_{3(g)}$ or $NO_{3\ (part)}^-$, we would expect to see larger differences between $\delta^{15}N$ values in the $HNO_{3(g)}$ and $NO_{3\ (part)}^-$ fractions during the warmer summer months. During the summer, $\delta^{15}N$-$NO_{3\ (part)}^-$ and $\delta^{15}N$-$HNO_{3(g)}$ values are most similar (average difference of 0.7‰) compared to other seasons where the difference can be up to 3.5‰. This suggests sampling artifacts do not cause large fractionations in $\delta^{15}N$ values. Further, the seasonal and spatial patterns we observe in the dry deposition fraction are similar to patterns in wet deposition that are free from such sampling artifacts.

5.3. Assessment of Passive Sampling for Isotopic Analysis

[47] At these CASTNET study sites, dry deposition of HNO_3 is the dominant form of dry inorganic nitrogen deposition measured by existing CASTNET methods (i.e., particulate nitrate plus nitric acid dry deposition), comprising between 70 and 80% of total dry inorganic nitrogen deposition (Table 1). Although further testing of the efficacy of passive samplers is warranted, our preliminary results demonstrate that passive collection of HNO_3 yields reproducible isotopic signatures for both $\delta^{15}N$ and $\delta^{18}O$ of HNO_3, as

indicated by the low standard deviations for replicate samples across multiple sites. Further, we observe only slight differences in $\delta^{15}N$ values between actively and passively collected HNO3 (0.6‰) suggesting that passive HNO_3 collection may be an effective surrogate for active collection procedures. However, the offset in $\delta^{18}O$ values between actively and passively collected samples is larger (6.4‰); the causes for this offset warrant further investigation ideally with comparisons over longer time periods and at multiple sites.

[48] These results suggest that passive collectors offer a novel, cost-effective medium for collection of dry nitrogen deposition for isotopic analysis, particularly for $\delta^{15}N$. While this study used HNO_3 samplers developed by the U.S. Forest Service [*Bytnerowicz et al.*, 2005], samplers have been developed based on low-cost, commercially available parts [*Golden et al.*, 2008]. Passive collectors provide a new opportunity to measure the spatial distribution of dry nitrogen deposition, with unprecedented ease and minimal costs. Although passive samplers can be problematic for estimating dry deposition rates due to the difficulties in measuring or estimating deposition velocities, they represent a significant advance in assessing concentration patterns, and now isotopic composition, at higher spatial resolutions than currently allowed by the sparse distribution of CASTNET sites. Given that HNO_3 deposition is a major component of dry nitrogen deposition, these samplers offer a new method for exploring the role of HNO_3 deposition to diverse landscapes, and ultimately the impact of dry deposition on ecosystems and water quality.

6. Conclusions and Implications

[49] In the largest-scale study of dry deposition isotopes conducted in the U.S.A. to date, we demonstrate that dry nitrogen deposition, including particulate nitrate and nitric acid, is significantly influenced by emissions from industrial stationary sources, such as electricity generating facilities. These results suggest that the isotopic composition of dry deposition can be used as an additional tool to help understand the NO_x sources that contribute to aerosol and gaseous N formation and ultimately deposition on the landscape. These results complement those recently published suggesting that the isotopic composition of wet nitrate deposition is a better predictor of the influence of stationary sources on precipitation chemistry than commonly used metrics for acidic deposition, including pH, sulfate and nitrate concentrations [*Elliott et al.*, 2007].

[50] Of particular interest, we determined that the isotopic composition of dry nitrogen deposition is not correlated with regional vehicle emissions surrounding individual CASTNET sites. These results suggest the possibility that mobile and stationary source NO_x emissions are subject to different fates in the environment, with potentially important implications for public and ecosystem health, as well as water quality. Future research should examine the fate of vehicle emissions in near road environments, and stable isotope tracers may be one effective means of doing this.

[51] Last, we demonstrate in a small-scale pilot study, that the passive collection of HNO_3 yields reproducible results with comparable $\delta^{15}N$ values as those collected using active sampling techniques. These results, although preliminary, indicate that passive sampling techniques can effectively be used as a medium for isotopic analysis. Although HNO_3 is the largest component of dry inorganic nitrogen deposition currently measured at CASTNET sites, future research should investigate the use of passive samplers for NO_2 and NH_3 collections, which are currently not measured at CASTNET sites. These techniques potentially open the door to many interesting questions regarding the spatial distribution of dry deposition to landscapes, and how the sources of these inputs vary spatially.

[52] **Acknowledgments.** We gratefully acknowledge laboratory assistance from Cecily Chang, Mark Rollog, and Steve Silva. We also thank Scott Wankel for his laboratory assistance and work with the microbial denitrifier method. We thank Michael Brown for his assistance in deployment of the passive samplers and in determining concentrations of eluted passive samples, and Dan Bain for his assistance with GIS. We are grateful to the CASTNET (MACTEC) and NADP staff for their cooperation in this study and assistance with receiving archived samples for isotopic analysis. We appreciate review comments from Robert Vet, Scott Wankel, and two anonymous reviewers that substantially improved this manuscript. This work was supported by grants from the New York State Energy Research and Development Authority, the Electric Power Research Institute, and the U.S. Geological Survey; we are especially grateful to Ellen Burkhard, Rick Carlton, and Mark Watson for their interest in this work and support of this effort. This paper has been reviewed in accordance with the U.S. Environmental Protection Agency's peer and administrative review policies and approved for publication. Approval does not signify that the contents necessarily reflect the views and policies of the agency, nor does the mention of trade names or commercial products constitute endorsement or recommendation for use.

References

Ames, R. B., and W. C. Malm (2001), Comparison of sulfate and nitrate particle mass concentrations measured by IMPROVE and the CDN, *Atmos. Environ.*, *35*(5), 905–916, doi:10.1016/S1352-2310(00)00369-1.

Ammann, M., et al. (1999), Estimating the uptake of traffic-derived NO_2 from N-15 abundance in Norway spruce needles, *Oecologia*, *118*(2), 124–131, doi:10.1007/s004420050710.

Ansari, A. S., and S. P. Pandis (2000), The effect of metastable equilibrium states on the partitioning of nitrate between gas and aerosol phases, *Atmos. Environ.*, *34*, 157–168, doi:10.1016/S1352-2310(99)00242-3.

Brown, S. S., et al. (2006), Variability in nocturnal nitrogen oxide processing and its role in regional air quality, *Science*, *311*, 67–70, doi:10.1126/science.1120120.

Butler, T. J., et al. (2005), The impact of changing nitrogen oxide emissions on wet and dry nitrogen deposition in the northeastern USA, *Atmos. Environ.*, *39*(27), 4851–4862, doi:10.1016/j.atmosenv.2005.04.031.

Bytnerowicz, A., et al. (2005), Passive sampler for monitoring ambient nitric acid (HNO_3) and nitrous acid (HNO_2) concentrations, *Atmos. Environ.*, *39*(14), 2655–2660, doi:10.1016/j.atmosenv.2005.01.018.

Calvert, J. G., et al. (1985), Chemical mechanisms of acid generation in the troposphere, *Nature*, *317*, 27–35, doi:10.1038/317027a0.

Casciotti, K. L., et al. (2002), Measurement of the oxygen isotopic composition of nitrate in seawater and freshwater using the denitrifier method, *Anal. Chem.*, *74*(19), 4905–4912, doi:10.1021/ac020113w.

Casciotti, K. L., et al. (2007), Oxygen isotopes in nitrite: Analysis, calibration, and equilibration, *Anal. Chem.*, *79*(6), 2427–2436, doi:10.1021/ac061598h.

Elliott, E. M., et al. (2007), Nitrogen isotopes as indicators of NO_x source contributions to atmospheric nitrate deposition across the midwestern and northeastern United States, *Environ. Sci. Technol.*, *41*(22), 7661–7667, doi:10.1021/es070898t.

Fenn, M. E., et al. (2003), Nitrogen emissions, deposition, and monitoring in the western United States, *BioScience*, *53*(4), 391–403, doi:10.1641/0006-3568(2003)053[0391:NEDAMI]2.0.CO;2.

Freyer, H. D. (1978), Seasonal trends of $NH_4(+)$ and $NO_3(-)$ nitrogen isotope composition in rain collected at Julich, Germany, *Tellus*, *30*(1), 83–92.

Freyer, H. D. (1991), Seasonal variation of $^{15}N/^{14}N$ ratios in atmospheric nitrate species, *Tellus, Ser. B*, *43*, 30–44.

Freyer, H. D., et al. (1993), On the interactions of isotopic exchange processes with photochemical reactions in atmospheric oxides of nitrogen, *J. Geophys. Res.*, *98*(D8), 14,791–14,796, doi:10.1029/93JD00874.

Garrett, T. J., et al. (2006), Quantifying wet scavenging processes in aircraft observations of nitric acid and cloud condensation nuclei, *J. Geophys. Res.*, *111*, D23S51, doi:10.1029/2006JD007416.

Garten, C. T. (1996), Stable nitrogen isotope ratios in wet and dry nitrate deposition collected with an artificial tree, *Tellus, Ser. B*, *48*, 60–64.

Gilbert, N. L., et al. (2002), Ambient nitrogen dioxide monitoring near a major highway using passive diffusion samplers, *Epidemiology*, *13*(4), S146–S147.

Gilbert, N. L., et al. (2003), Ambient nitrogen dioxide and distance from a major highway, *Sci. Total Environ.*, *312*(1–3), 43–46, doi:10.1016/S0048-9697(03)00228-6.

Golden, H. E., et al. (2008), Simple approaches for measuring dry atmospheric nitrogen deposition to watersheds, *Water Resour. Res.*, *44*, W00D02, doi:10.1029/2008WR006952.

Hastings, M. G., et al. (2003), Isotopic evidence for source changes of nitrate in rain at Bermuda, *J. Geophys. Res.*, *108*(D24), 4790, doi:10.1029/2003JD003789.

Hastings, M. G., et al. (2004), Seasonal variations in N and O isotopes of nitrate in snow at Summit, Greenland: Implications for the study of nitrate in snow and ice cores, *J. Geophys. Res.*, *109*, D20306, doi:10.1029/2004JD004991.

Hastings, M. G., et al. (2005), Glacial/interglacial changes in the isotopes of nitrate from the Greenland Ice Sheet Project 2 (GISP2) ice core, *Global Biogeochem. Cycles*, *19*, GB4024, doi:10.1029/2005GB002502.

Heaton, T. H. E. (1987), 15N/14N ratios of nitrate and ammonium in rain at Pretoria, South Africa, *Atmos. Environ.*, *21*(4), 843–852, doi:10.1016/0004-6981(87)90080-1.

Heaton, T. H. E. (1990), 15N/14N ratios of NO_x from vehicle engines and coal-fired power stations, *Tellus, Ser. B*, *42*, 304–307.

Hicks, B. B., et al. (1987), A preliminary multiple resistance routine for deriving dry deposition velocities from measured quantities, *Water Air Soil Pollut.*, *36*, 311–330, doi:10.1007/BF00229675.

Hoering, T. (1957), The isotopic composition of the ammonia and the nitrate ion in rain, *Geochim. Cosmochim. Acta*, *12*(1–2), 97–102, doi:10.1016/0016-7037(57)90021-2.

Hudman, R. C., et al. (2007), Surface and lightning sources of nitrogen oxides over the United States: Magnitudes, chemical evolution, and outflow, *J. Geophys. Res.*, *112*, D12S05, doi:10.1029/2006JD007912.

Jaegle, L., et al. (2005), Global partitioning of NO_x sources using satellite observations: Relative roles of fossil fuel combustion, biomass burning and soil emissions, *Faraday Discuss.*, *130*, 407–423, doi:10.1039/b502128f.

Jarvis, J. C., et al. (2008), Influence of local photochemistry on isotopes of nitrate in Greenland snow, *Geophys. Res. Lett.*, *35*, L21804, doi:10.1029/2008GL035551.

Johnston, J. C., and M. H. Thiemens (1997), The isotopic composition of tropospheric ozone in three environments, *J. Geophys. Res.*, *102*(D21), 25,395–25,404, doi:10.1029/97JD02075.

Kiga, T., et al. (2000), Evaluation of NO_x formation in pulverized coal firing by use of nitrogen isotope ratios, paper presented at International Joint Power Generation Conference, Am. Soc. of Mech. Eng., Miami Beach, Fla., 23–26 July.

Krankowsky, D., et al. (1995), Measurement of heavy isotope enrichment in tropospheric ozone, *Geophys. Res. Lett.*, *22*(13), 1713–1716, doi:10.1029/95GL01436.

Krupa, S. V., and A. H. Legge (2000), Passive sampling of ambient, gaseous air pollutants: An assessment from an ecological perspective, *Environ. Pollut.*, *107*, 101–137, doi:10.1016/S0269-7491(99)00154-2.

Li, D., and X. Wang (2008), Nitrogen isotopic signature of soil-released nitric oxide (NO) after fertilizer application, *Atmos. Environ.*, *42*, 4747–4754, doi:10.1016/j.atmosenv.2008.01.042.

Liang, J. Y., et al. (1998), Seasonal budgets of reactive nitrogen species and ozone over the United States, and export fluxes to the global atmosphere, *J. Geophys. Res.*, *103*(D11), 13,435–13,450, doi:10.1029/97JD03126.

Michalski, G., et al. (2003), First measurements and modeling of Delta O-17 in atmospheric nitrate, *Geophys. Res. Lett.*, *30*(16), 1870, doi:10.1029/2003GL017015.

Moore, H. (1977), The isotopic composition of ammonia, nitrogen dioxide, and nitrate in the atmosphere, *Atmos. Environ.*, *11*, 1239–1243, doi:10.1016/0004-6981(77)90102-0.

Morin, S., et al. (2008), Tracing the origin and fate of NO_x in the arctic atmosphere using stable isotopes in nitrate, *Science*, *322*(5902), 730–732, doi:10.1126/science.1161910.

Morino, Y., et al. (2006), Partitioning of HNO_3 and particulate nitrate over Tokyo: Effect of vertical mixing, *J. Geophys. Res.*, *111*, D15215, doi:10.1029/2005JD006887.

NARSTO (2005), Improving emission inventories for effective air quality management across North America—A NARSTO assessment, Pasco, Wash.

National Atmospheric Deposition Program Central Analytical Laboratory (2006), Standard operating procedure for the determination of Cl, NO_3, and SO_4 using Dionex DX-500 ion chromatography and Chromeleon software, Ill. State Water Surv., Champaign.

Neuman, J. A., et al. (2006), Reactive nitrogen transport and photochemistry in urban plumes over the North Atlantic Ocean, *J. Geophys. Res.*, *111*, D23S54, doi:10.1029/2005JD007010.

Ozden, O., and T. Dogeroglu (2008), Field evaluation of a tailor-made new passive sampler for the determination of NO_2 levels in ambient air, *Environ. Monit. Assess.*, *142*(1–3), 243–253, doi:10.1007/s10661-007-9921-x.

Pearson, J., et al. (2000), Traffic exposure increases natural ^{15}N and heavy metal concentrations in mosses, *New Phytol.*, *147*(2), 317–326, doi:10.1046/j.1469-8137.2000.00702.x.

Plaisance, H., et al. (2002), Performances and application of a passive sampling method for the simultaneous determination of nitrogen dioxide and sulfur dioxide in ambient air, *Environ. Monit. Assess.*, *79*(3), 301–315, doi:10.1023/A:1020205230396.

Rabaud, N. E., et al. (2001), A passive sampler for the determination of airborne ammonia concentrations near large-scale animal facilities, *Environ. Sci. Technol.*, *35*(6), 1190–1196, doi:10.1021/es0012624.

Roadman, M. J., et al. (2003), Validation of Ogawa passive samplers for the determination of gaseous ammonia concentrations in agricultural settings, *Atmos. Environ.*, *37*(17), 2317–2325, doi:10.1016/S1352-2310(03)00163-8.

Sather, M. E., et al. (2007), Evaluation of Ogawa passive sampling devices as an alternative measurement method for the nitrogen dioxide annual standard in El Paso, Texas, *Environ. Monit. Assess.*, *124*(1–3), 211–221, doi:10.1007/s10661-006-9219-4.

Saurer, M., et al. (2004), First detection of nitrogen from NO_x in tree rings: A N-15/N-14 study near a motorway, *Atmos. Environ.*, *38*(18), 2779–2787, doi:10.1016/j.atmosenv.2004.02.037.

Savarino, J., et al. (2007), Nitrogen and oxygen isotopic constraints on the origin of atmospheric nitrate in coastal Antarctica, *Atmos. Chem. Phys.*, *7*(8), 1925–1945.

Schaap, M., et al. (2004), Artefacts in the sampling of nitrate studied in the "INTERCOMP" campaigns of EUROTRAC-AEROSOL, *Atmos. Environ.*, *38*(38), 6487–6496, doi:10.1016/j.atmosenv.2004.08.026.

Seinfeld, J. H., et al. (1998), *Atmospheric Chemistry and Physics: From Air Pollution to Climate Change*, 1326 pp., Wiley, New York.

Sigman, D. M., et al. (2001), A bacterial method for the nitrogen isotopic analysis of nitrate in seawater and freshwater, *Anal. Chem.*, *73*(17), 4145–4153, doi:10.1021/ac010088e.

Wankel, S. D., et al. (2009), Sources of aerosol nitrate to the Gulf of Aqaba: Evidence from d15N and d18O of nitrate and trace metal chemistry, *Mar. Chem.*, in press.

Wesely, M. L., and B. B. Hicks (2000), A review of the current status of knowledge on dry deposition, *Atmos. Environ.*, *34*(12–14), 2261–2282, doi:10.1016/S1352-2310(99)00467-7.

Wolfe, A. P., et al. (2001), Anthropogenic nitrogen deposition induces rapid ecological changes in alpine lakes of the Colorado Front Range (USA), *J. Paleolimnol.*, *25*(1), 1–7, doi:10.1023/A:1008129509322.

Wolfe, A. P., et al. (2003), Recent ecological and biogeochemical changes in alpine lakes of Rocky Mountain National Park (Colorado, USA): A response to anthropogenic nitrogen deposition, *Geobiology*, *1*, 153–168, doi:10.1046/j.1472-4669.2003.00012.x.

E. W. Boyer, School of Forest Resources, Pennsylvania State University, University Park, PA 16802, USA.

D. A. Burns, U.S. Geological Survey, Troy, NY 12180, USA.

T. J. Butler, Department of Ecology and Evolutionary Biology, Cornell University, Ithaca, NY 14853, USA.

A. Bytnerowicz, U.S. Forest Service, Riverside, CA 92507, USA.

E. M. Elliott, Department of Geology and Planetary Science, University of Pittsburgh, 200 SRCC, 4107 O'Hara Street, Pittsburgh, PA 15260, USA. (eelliott@pitt.edu)

R. Glatz, San Francisco, CA 94117, USA.

H. E. Golden, U.S. Environmental Protection Agency, Athens, GA 30605, USA.

K. Harlin, Central Analytical Laboratory, National Atmospheric Deposition Program, Champaign, IL 61820, USA.

C. Kendall, U.S. Geological Survey, Menlo Park, CA 94025, USA.

G. G. Lear, U.S. Environmental Protection Agency, Washington, DC 20460, USA.